https://doi.org/10.15407/scine18.01.112

VOROPAI, A. (https://orcid.org/0000-0002-2783-6700),
and **SARANA, V.** (https://orcid.org/0000-0002-7778-3176)
Oles Honchar Dnipro National University,
72, Haharina Ave, Dnipro, 49000, Ukraine,
+380 56 374 9822, cdep@dnu.dp.ua

LOW-NOISE AND COST-EFFECTIVE ACTIVE ELECTRODES FOR DRY CONTACT ECG APPLICATIONS

Introduction. *Active ECG electrodes for daily usable wearable electronics (glasses, headphones) enable making long-term cardiovascular disease diagnostics available to many people.*

Problem Statement. *The methods of ECG recording become more accessible over the years. However, on the way to their general use, even in cases where only reliable registration of the R-wave of the ECG is important, there are certain difficulties associated with the need to apply special electrodes (eg, silver chloride ones) to certain parts of the body through wet pads and to perform specific actions.*

The problem is solved by using dry electrodes built into the usual devices. However, in this case, a low amplitude of the useful signal and a high contact resistance (for example, on the surface of the head) do not allow recording an ECG by conventional means.

Purpose. *The purpose of this research is to develop easy-to-use body ECG electrodes that may be built into everyday appliances.*

Materials and Methods. *Active electrodes based on flexible conductive materials and high-quality operational amplifiers have been described. The main parameters of the electronic circuit have been obtained by model and experimental research. The parameters have been compared with the corresponding characteristics of commercial samples.*

Results. *Prototype active ECG electrodes have been developed, created, and studied. The obtained results have shown that the dependence of the input reactance on the frequency plays an important role in terms of the final signal quality. For a low-amplitude ECG signal, the prototype has shown a signal-to-noise ratio that is higher by 4.7 dB than that for high-quality commercial electrodes.*

Conclusions. *The designed electrodes may be used in body devices, on the body parts with a low amplitude of the useful signal and a high resistance of skin-electrode contact.*

Keywords: ECG, active electrodes, dry contact.

According to the World Health Organization, cardiovascular diseases (CVDs) are the most common cause of death worldwide. About 31% of death toll in 2016 was caused by CVDs [1]. The number of these fatal cases may be significantly reduced by regularly monitoring of the heart rate, in particular by recording the ECG in everyday life routine.

Citation: Voropai, A., and Sarana, V. (2022). Low-Noise and Cost-Effective Active Electrodes for Dry Contact ECG Applications. *Sci. innov.*, 18(1), 112—123. https://doi.org/10.15407/scine18.01.112

Typically, wet electrodes with an electrically conductive gel between the skin surface and electrodes made of Ag/AgCl are used for clinical and research needs. Sometimes the skin surface needs to be prepared or even shaved before applying the electrode to the skin. This is necessary to achieve the lowest contact resistance and the best signal-to-noise ratio of the recorded signal and to disregard the motion artifacts for preserving the shape of the QRS complex, P and W waves for the further analysis by specialists or automated systems. However, such a signal quality is not required for home use, fitness or sports, where recording an ECG with a clinical signal quality level can be very difficult because of the limited shelf life of wet electrodes, the relatively complicated and inconvenient process of connecting passive electrodes. It is especially relevant during long recordings, when wet electrodes may start to get dried on warm skin, which significantly increases the contact resistance with the skin and reduces the signal-to-noise ratio. The surface of the patient's skin may become irritated, itchy, red, and even suffer from an allergic reaction [2]. Electrodes with a dry skin contact are increasingly being used to address these problems. Dry electrodes greatly simplify the ECG signal recording, making this process more accessible to ordinary users. Such electrodes may be made of special flexible textiles that conduct electricity. This allows integrating them into everyday household items, such as clothing [3], glasses, headphones, furniture [4, 5, 6, 7] or even seat belts and car driver seats [8, 9]. One of the significant differences between wet and dry electrodes is that in the case of the use of dry electrodes, the skin-electrode contact improves over time as compared with worsening contact in the case of wet electrodes [10].

Nevertheless, the dry electrodes have their drawbacks, such as: a high resistance of the electrode-skin contact as compared with the wet electrodes and a high sensitivity to motion artifacts. The high skin contact resistance may be compensated by increasing the input resistance of the electrode by using active electrodes with a built-in field-effect transistor or operational amplifier (OpAmp). The sensitivity to motion artifacts may be reduced by using active electrodes with a built-in accelerometer [11, 18] and additional pulse wave removal methods, for example photoplethysmography (PPG) [12] or ballistocardiography (BCG) [13] to increase the chances of registration of R-peaks in a noisy signal.

Starting with 1887, when the first ECG was published by D. Waller [14], and until 1964, saline was a mandatory component for ECG recordings as an electrolyte. This was because of the input resistance of the cardiographs in several MOhm and the observance of traditions. As late as in 1964, D. Lewes [15] tried to record an ECG without the use of electrolyte and without careful preparation of the skin before wearing passive electrodes. Four years later, isolated dry electrodes made of anodized aluminum and a field-effect transistor, as a converter of input impedance that exceeded 1 TOhm were introduced [16].

Since then, the quality of ECG recording with the use of dry electrodes has improved significantly. According to T. Kosierkiewicz [17], the dry electrodes made of a mix of silicone and silver filler may outperform classic the wet electrodes, providing less resistance between the skin and the electrode. In addition to silicone, the leading interface may be a fabric with the addition of a thin metal thread. In [18], Xiang An та George K. Stylios have presented the optimal dry electrodes based on textiles in the size of 2×4 cm, which allow recording an ECG with as good quality of a signal as in the case of the wet electrodes. In addition to that, there are methods for taking an ECG even without any contact with skin.

Active electrodes may be divided into the two types: the contactless (or insulated) and the contact (or non-insulated) electrodes. In the case of contactless electrodes, biopotentials are measured remotely at a distance from several tenths of a mm to one meter [23]. The input impedance may reach POhms. However, the input of such electrodes acts as an antenna that receives any surroundings electric and magnetic fields, which leads to decreasing

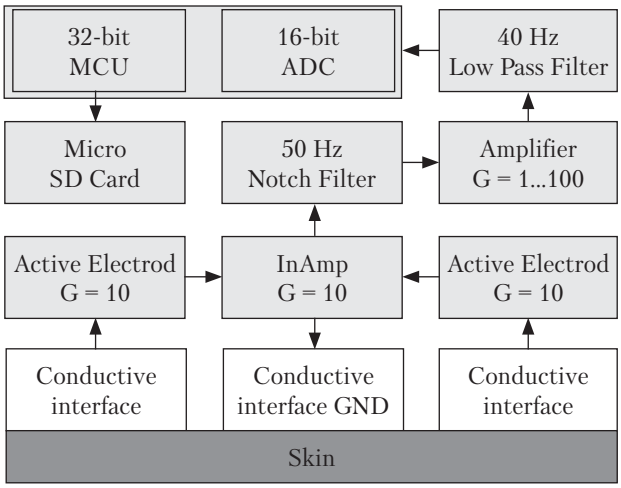

Fig. 1. Block diagram of the ECG recording system

of the signal-to-noise ratio. In addition, often the contactless electrodes do not have amplification at all, which requires an additional amplifier. The active contact electrodes have a much lower input impedance with an upper limit of up to tens GOhm [24], they are in a galvanic contact with the skin. There may be resistors or capacitors connected in series between the skin and the input of the amplifier. If they are input capacitors, such electrodes are called AC-Coupled, if, instead of capacitors, resistors are used, such electrodes are DC-Coupled. The AC-Coupled electrodes allow removing the bias voltage, this enables increasing the gain of the first stage, but, on the other hand, it reduces the input resistance. In this research, our own circuit of the active AC-Coupled electrodes using free software and entry-level tools has been developed.

The purpose of this research is to develop a prototype active electrodes for ECG recording from the surface of the human scalp at low signal levels, which makes sense when embedding ECG recording in everyday appliances, such as headphones or glasses. To achieve this goal, it is necessary to solve the following tasks:

- to build a basic scheme of the active electrode circuit;
- to calculate the frequency of the built-in bandpass filter;
- to make model studies of the circuit;
- to build the first prototype of the designed circuit;
- to measure the actual characteristics of the prototype;
- to build an installation for experimental studies of the main characteristics and parameters of the prototype;
- to check in practice the operability of the designed device by recording ECG signals from the temporal parts of the head in different people;
- to compare the designed solution with modern high-quality commercial active ECG electrodes.

The existing commercial electrocardiographs have a signal amplification factor, usually up to 200 V/V. This is not enough to record the signal from the surface of the scalp since such a signal needs to be amplified 7000—10000 times [25]. A modular recording system has been created to record such a weak signal.

The recording system consists of a microcontroller, active electrodes under test, an instrument amplifier, filters, and an amplifier for matching the resistance and an input voltage range of the ADC (Fig. 1).

The recording system is based on CoreH743I board made by Waveshare Electronics. STM32H743IIT6 ARM Cortex-M7 microcontroller from STMicroelectronics is installed on this board. Microcontrollers STM32H7 have the three successive approximation registers (SAR) ADC with 16-bits resolution, 77 dB signal-to-noise ratio (SNR), and 87 dB Total Harmonic Distortion (THD) for single-ended ADC [26, 27]. To get the effective number of bits (ENOB), this ADC SINAD (signal-to-noise and distortion ratio) shall be calculated first, with the use of formula (1). After the SINAD calculation, ENOB may be found from formula (2). It gives around 12.4 bits ENOB. It more than two bits higher than the ENOB STM32F7 family microcontrollers that provide 10.4 bits for 12 bits ADC, 65 dB SNR and 72 dB THD [28].

$$\text{SINAD} = -10\log_{10}\left(10^{-\text{SNR}/10} + 10^{-\text{THD}/10}\right). \quad (1)$$

Where SINAD is signal-to-noise and distortion ratio, SNR is signal-to-noise ratio, THD is total harmonic distortion.

$$\text{ENOB} = \frac{\text{SINAD} - 1.76}{6.02}. \quad (2)$$

Where ENOB is effective number of bits, SINAD is signal-to-noise-and-distortion.

To increase SNR of the microcontroller ADC, the oversampling method is used. Oversampling or averaging 4 samples to one sample improves SNR by 5 dB, which may theoretically increase ENOB from 12.4 to 13.1 bits. With this resolution, the embedded ADC of the microcontroller may be used to record ECG signal.

A special amplifier based on Microchip MCP6024 has been created to amplify the ECG signal. MCP6024 has 2.5—5.5 V power supply range, 500 uV input offset, wide common-mode input range from VSS — 0.3 to VDD + 0.3, low THD 0.005%, 2.9 uVpp input noise at 0.1—10 Hz, and 60 nV/√Hz input noise voltage density at 10 Hz.

The created amplifier contains a notch filter with –80 dB rejection of 50 Hz mains interference noise and low pass filter with cut-off frequency of 40 Hz. The combination of these filters makes a roll-off frequency response with a 40 dB per decade slope. This filter configuration ensures the removal of high-frequency noise, as well as mains interferente noise and unwanted biosignals such as electromyographic noise which appears at 10 Hz and reaches several hundred Hz [29].

The cutoff frequencies of the filters are chosen on the basis of several factors. The first of them is the frequency of the power line of the country where the experiments are carried out, and the second is the known frequency spectrum of the ECG signal. According to M. Allen [30] who was one of the first researhers to calculate the frequency spectrum of ECG signals 60 years ago, more that 98% of the total spectrum does not exceed 90 Hz. In 1984, V. Thakor, G. Webster, and J. Tompkins [31] have developed a selective filter with a center frequency of 17 Hz and a quality factor (Q) = 5 to maximize the amplitude of R peaks.

According to the Nyquist — Shannon — Kotelnikov theorem, the sampling frequency of the recording system shall be two or more times higher than the component of the maximum frequency of the recorded analog signal to be able to recover all recorded information. Therefore, an 80 Hz sampling rate is sufficient to collect basic information about the QRS complex, but most existing electrocardiographs have a sampling rate up to 500 Hz to record all information from the high-frequency components of ECG signal. For this research, we use a sampling rate of 1000 Hz (4000 Hz for quadratic oversampling) to be able to record R peaks with an accuracy of up to 1 ms for future HRV analysis. The amount of generated data is 2000 bytes per second, or 120 KB per minute. A 2 GB SD card connected to the microcontroller via the SDIO interface is used to store the raw recorded data. The C/C ++ programming language is used to develop STMH743IIT6 microcontroller software. STM32CubeIDE provided by STMicroelectronics is chosen as IDE (integrated development environment). The STM32CubeMX graphical configuration tool is used to configure all 178 pins of the STMH743IIT6 microcontroller.

Skin-Electrode Contact

According to Xiang An and George K. Stylios [18], flexible textile fabric with integrated silver threads may provide contact quality at the level of standard wet electrodes. Therefore, as a conductive interface between the skin and the active electrodes, a similar flexible textile material is used, but with a Ni/Cu coating that has similar properties but is much cheaper. Achieved skin-electrode contact impedance is 10—15 MOhm after electrode installation and drops to 5—8 MOhm in a few minutes.

Development of Active ECG Electrodes

The nature of biosignals, such as ECG, EMG or EEG, requires a fairly wide range of supply voltage of the active electrodes. This is usually a bipolar power supply. In this research, two CR2032 batteries with a maximum voltage of 3 V are used

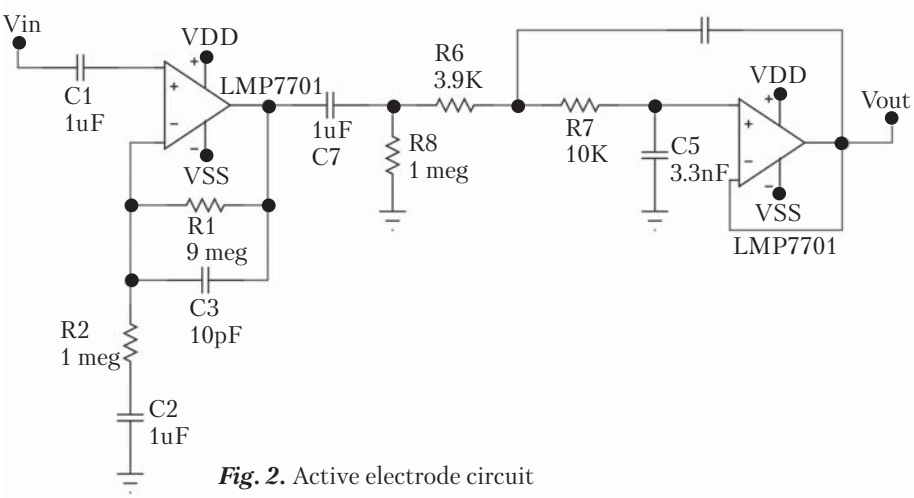

Fig. 2. Active electrode circuit

as a power source for the active electrodes. LMP7702, a dual amplifier, is chosen as the basis of the active electrodes because of a high input resistance, an ultra-low noise, and a wide range of supply voltage and input voltage.

The purpose of creating active electrodes in this research is to measure the ECG from non-standard leads of the human body, such as the Mastoid Area, the temporal bone behind the ears. The main frequency components of the ECG signal usually range within 0.1—100 Hz. Anything that exceeds this frequency range may be considered potential noise. Based on this, it has been decided to built-in a bandpass filter to eliminate all types of noise as soon as possible before the signal arrives at the input of the instrument amplifier.

The cutoff frequency of the low-pass filter should be approximately 100 times higher than the frequency of the useful signal to prevent a decrease in the amplitude of the useful signal. In turn, the cutoff frequency of the high-pass filter should be 100 times less than the frequency of the useful signal. It has been assumed that the central useful frequency of the ECG signal is 20 Hz. Therefore, the frequency range of the bandpass filter is from 0.2 Hz to 2 KHz. This frequency range allows us to ignore the DC voltage offset and to reject the main frequency components of the ECG without a significant distortion. Formulas (4) and (5) are used to find the required components and cutoff frequencies of the bandpass filter, and formula (1) is used to find the gain.

Micro-Cap 12 software is used to model the active electrode circuits. The active electrode diagram drawn with the *Micro-Cap 12* circuit editor is shown on Fig. 2.

The *Micro-Cap 12* modelling tool allows a comprehensive analysis of the circuit. It is used to simulate the operation of active electrodes on AC currents and to obtain the frequency characteristics (Figs. 3 and 4) and the dependence of the input resistance on frequency of an input signal with added parasitic capacitance and resistance (Fig. 5). The spectral noise density is calculated as well (Fig. 6).

$$A_V = 1 + \mathrm{R1}/\mathrm{R2}. \quad (3)$$

Where A_V is electrode gain.

$$F_{HPF} = \frac{1}{2\pi\sqrt{\mathrm{R2R8C2C7}}}. \quad (4)$$

Where F_{HPF} is the cutoff frequency of the high frequency filter.

$$F_{LPF} = \frac{1}{2\pi\sqrt{\mathrm{R2C3}}\ \sqrt{2\pi\mathrm{R6R1C5C6}}}. \quad (5)$$

Where F_{LPF} is the cutoff frequency of the low pass filter.

The active electrodes (Fig. 2) do not have a return path for the bias current because OpAmp LMP7702 has a very low bias current of 200 fA, which allows the circuit to operate for approxi-

mately 15 days continuously before entering the saturation mode to one of the two supply voltages. This scenario is not possible in this case, because the operation time of the circuit is limited to 8 working hours of the laboratory.

To avoid the problem of saturation of OpAmp, there are several known methods such as the use of a transistor switch [19] that may be activated when detecting the saturation mode on the output of the circuit. There is also a way to use inverted diodes [20] or to use the disadvantages of printed circuit boards to provide a small parasitic current [21]. The same effect may be achieved by wrapping an enameled wire around the OpAmp input [22]. In the further research, we will use one of these methods to manufacture the next version of the active electrodes.

Measurement of Amplitude-Frequency Characteristics and Input Resistance of Active Electrodes

The main characteristics of the active electrodes include gain, amplitude-frequency response, and input resistance. Measurement of these characteristics allows us to compare the designed electrodes with analogs. To this end, an automated testing system to measure characteristics of the active electrodes has been built (Fig. 7). An arbitrary signal generator FY6800 with a maximum frequency of the generated signal of 20 MHz and a USB interface is used as an input signal generator. *Rigol* DS1054Z digital oscilloscope is used as an oscilloscope to measure the output signal of the test electrode (device under test (DUT)).

In order to measure the input resistance of the electrodes, a switchable resistance Rt from 0 to 100 MOhm is included in the testing circuit. This allows us to measure the amplitude-frequency response of the electrode with a closed Rt (Rt = 0) and the input resistance at maximum Rt (Rt = = 100 MOm) with the use of formula (6).

To reduce the amplitude of the induced external noise, the active electrodes, the resistor Rt, and the batteries of the active electrodes are placed in a Faraday cage made of 10-layer aluminum film

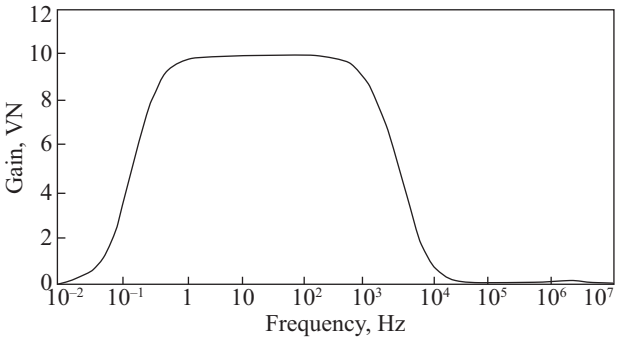

Fig. 3. Frequency response obtained by simulation

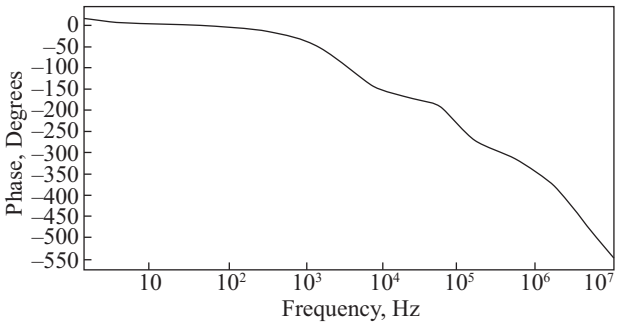

Fig. 4. Phase response obtained by simulation

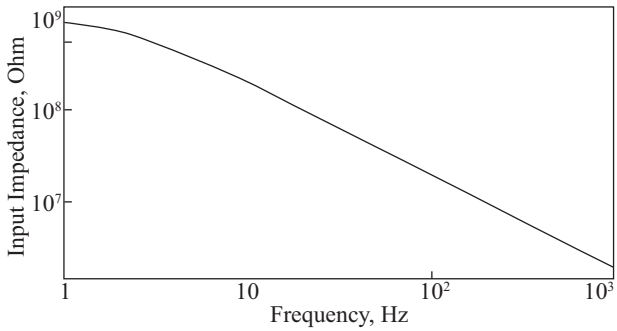

Fig. 5. Dependence of input resistance on frequency of the model

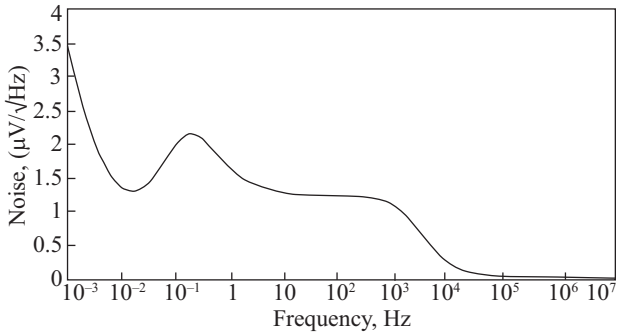

Fig. 6. Spectral density of noise power of the model

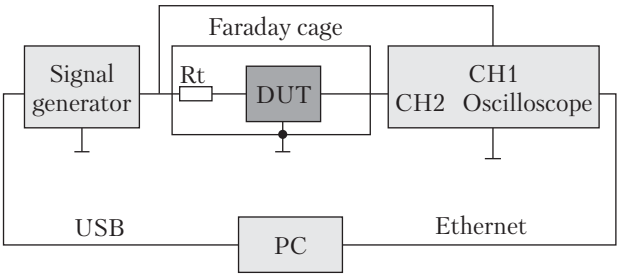

Fig. 7. Block diagram of the automated testing system. (Where DUT is device under test, PC is personal computer)

and cardboard. The conductive surface of the Faraday cage is connected to the ground of the system.

To automate long-term measurements, a signal generator and an oscilloscope are connected to a personal computer that controls the process via USB and Ethernet by executing scripts described in the Python programming language. This software is based on modified project DS1054Z_BodePlotter [34] and FY6XXX library. This project enables measuring the frequency response at a frequency of 0.01 Hz and calculating the input resistance of the DUT.

$$R_{IN} = R_t \left(\frac{\frac{V_2}{A_V(F)}}{V_1 - \frac{V_2}{A_V(F)}} \right). \quad (6)$$

The formula for calculating the input resistance of the active electrode given the non-uniformity of the frequency response of the active electrodes.

Where R_{IN} input resistance, $A_V(F)$ is the measured gain of the electrode at a specific frequency F, V_2 is the obtained voltage amplitude of the signal generator, V_2 is the obtained amplitude of the output voltage of the electrode.

Recording of ECG

Recording a standard ECG from human limbs is a well-studied process that may be performed with the use of passive electrodes without active electrodes and primary amplification of a signal. Recording an ECG from the scalp is more complicated and interesting from the point of view of wearable electronics, which requires the use of active electrodes with high input resistance and gain, because the ECG voltage on the scalp is about tens of μV, as compared with mV in standard ECG.

Winokur [25] has shown that the optimal place to record the ECG from the surface of the head is the Mastoid Area of the temporal bone behind the ears. We use this place for real-world tests of active electrodes and ECG recording for the experiment.

ECG signal is recorded for a group of 5 patients, 3 women and 2 men with an age from 25 to 53 years. Two active electrodes are located on the temporal bones of the skull behind the ears on both sides of the head. Each electrode has two contacts with the skin, the signal and the ground. The signal is recorded on the subjects under the same conditions, with the same settings of the gain, frequencies of analog and digital filters of the system. During the recordings, we change only the active electrodes (the commercial samples (Plessey PS25255) and the electrodes of own design based on OpAmp LMP7702) and the head position.

Data Processing

The collected data has been analyzed with the use of PyCharm Community Edition IDE with Anaconda plugin, free to use IDE (integrated development environment), and Python programming language. Each recorded ECG signal is filtered by a digital bandpass filter with a frequency range from 5 to 30 Hz to isolate the main frequency components of the signal.

To obtain the signal-to-noise ratio of recordings, the modified Pan-Thomkins algorithm in Python programming language [32] has been used for registering R-peaks. This allows the amplitude of the signal and the amplitude of the noise to be calculated automatically to find the signal-to-noise ratio by formula (7).

$$\mathrm{SNR} = 20\log_{10} \frac{A_s}{A_n}. \quad (7)$$

Where A_s is amplitude of a signal, A_n is amplitude of a noise.

Measured Gain and Frequency Response of Active Electrodes

Fig.8. features the frequency response of the active electrodes as obtained by the automated testing system. The obtained data show the difference between the practical frequency response and the simulated frequency response of the designed active electrodes (Fig. 8).

The first difference is the gain error because of the specific selection of resistors in the feedback circuit. The second difference is the error of 10% and 20% of the capacitors in the network of low-pass filters. They are selected in pairs to match each other in each of the two electrodes. The frequency response of the high-pass filter perfectly matches the computer model.

The Plessey PS25255 gain error is 15% and provides only 8.5 V/V gain out of the required 10 V/V from the Plessey Semiconductor datasheets [33].

Our experimental data have indicated that the cutoff frequency of PS25255 electrodes is 350 kHz, as compared with 20 kHz from the datasheets. They also have an undocumented frequency response unevenness of about 2 V/V that is approximately 25% of the total gain.

Input Resistance of Active Electrodes

Fig. 9 shows the results of measuring the input resistance of the electrodes. The measured impedance of the electrodes PS25255 is 15 GOhm at a frequency of 10 Hz, as compared with 260 MOhm for the electrodes based on OpAmp LMP7702 with the same frequency (Table 1). However, at a frequency of 100 Hz, the input resistance of the

Table 1. **Measured Input Resistance of the Active Electrodes**

Frequency, Hz	Input impedance, MOhm	
	PS25255	LMP7702
1	37000	736
10	15000	260
100	300	110
1000	20	6.5

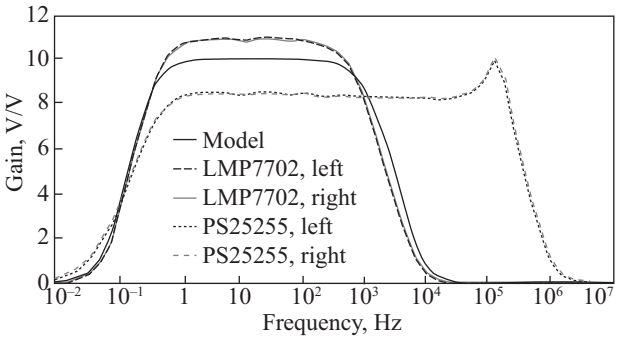

Fig. 8. Frequency response of electrodes

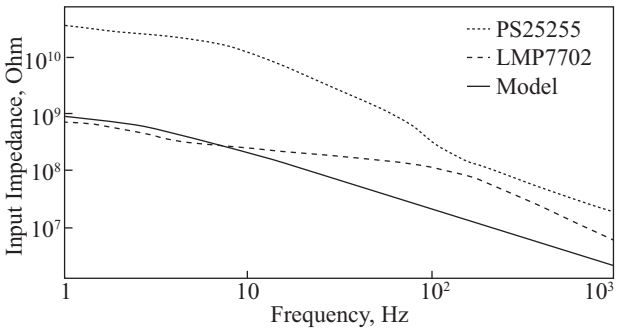

Fig. 9. Input resistance of the active electrodes based on OpAmp LMP7702 and commercial PS25255

active electrodes PS25255 drops 50 times as compared with a 2.36-times decrease for the electrodes based on OpAmp LMP7702, which indicates a significant advantage of the latter in this respect.

ECG Recording from the Surface of a Human Head

Measurement type 1 (Table 2) corresponds to the sitting body positions where the muscles of the neck and the back do respond to the load and cause noise in the ECG signals. Measurement types 2 and 3 correspond to the position of the head placed on a headrest, which increases the reduction of the noise amplitude and improves the signal-to-noise of the recorded signal.

Fig. 10 shows a view of the ECG signal recorded from the surface of the scalp. As one can see from the graph, the maximum amplitude of the useful signal obtained from the electrodes PS25255 is about 200 μV that is 16.5 times higher than the amplitude of the signal obtained from the desig-

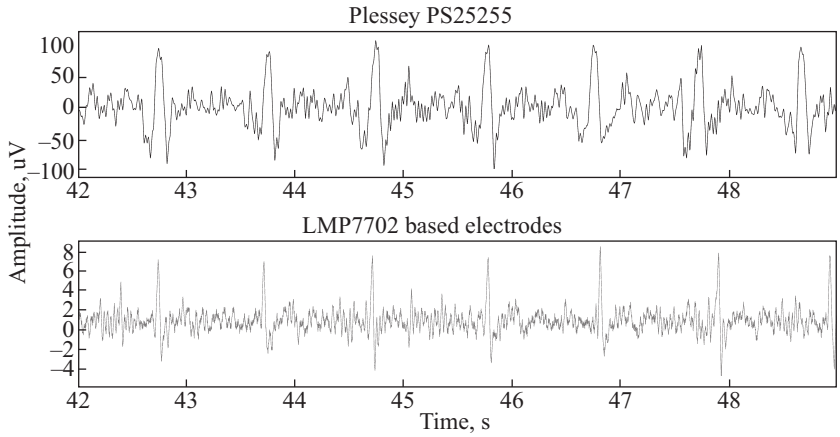

Fig. 10. View of ECG signal recorded from electrodes placed on the temporal parts of the head

ned OpAmp LMP7702 based electrodes. This confirms the results of the measured input resistance of the electrodes at frequencies between 10 and 20 Hz. In this case, the recorded signal for a group of people indicates the advantage of the designed electrodes in terms of signal-to-noise ratio. The designed electrodes do not have a large distortion of the QRS complex of the ECG signal and allow detecting the R peaks with greater accuracy than the signal obtained from the commercial electrodes.

Table 2. **Measured Signal-To-Noise Ratio of the Active Electrodes**

Number	Subject	Type	Mean SNR (SD), dB	
			Plessey	LMP7702
1	1	1	7.04 (2.83)	10.43 (3.04)
2	1	2	7.04 (2.91)	13.97 (3.83)
3	1	3	9.18 (3.54)	11.28 (4.63)
4	2	1	6.44 (2.56)	17.0 (3.6)
5	2	2	7.46 (2.66)	16.41 (4.11)
6	2	3	9.89 (3.11)	15.96 (4.11)
7	3	1	6.3 (2.68)	7.12 (2.65)
8	3	2	8.01 (3.56)	9.34 (2.83)
9	3	3	6.8 (3.1)	7.54 (2.93)
10	4	1	5.41 (1.82)	16.87 (2.22)
11	4	2	5.86 (2.2)	18.3 (1.98)
12	4	3	7.38 (3.72)	17.81 (1.96)
13	5	1	10.75 (4.06)	13.37 (2.12)
14	5	2	7.79 (3.9)	12.55 (1.71)
15	5	3	7.74 (3.69)	14.93 (1.97)

The gain of the designed electrodes, as measured experimentally, is 11 V/V, as compared with 10 V/V obtained on the model. This 10% gain error is explained by the specific selection of feedback resistors R1 and R2. The pair of built-in electrodes has the appropriate components. The accuracy of resistors is about 0.1%, that of capacitors is about 1%.

Although the Plessey PS25255 has a higher input resistance and a higher amplitude of the output signal, the overall SNR of the recorded signal is slightly better in the case of the designed electrodes. The difference in SNR may be explained by a huge input impedance of PS25255 that acts as an antenna.

Uneven input resistance of the active electrodes Plessey PS25255 leads to a distorted shape of the QRS complex. Higher input resistance (15 TOhm) of the electrodes at low frequencies within tens of Hertz, as compared with lower input resistance (300 MOhm) in hundreds of Hertz, leads to a significant increase in the amplitude of the low-frequency components of the signal. Thus, the effect of the low-pass filter manifestes itself, as the R-peak becomes several times wider than it actually is. The proposed active electrodes based

on the OpAmp LMP7702 have a more uniform input resistance depending on the frequency (Fig. 9) than the PS25255 electrodes. This ensures uniform amplification of all frequency components of the signal. Also the designed electrodes have a linear phase response (Fig. 4) in the frequency range of the useful signal and a low noise level (Fig. 6) that provides high-quality signal recording.

Despite a relatively low input resistance of the designed electrodes, they have a better signal-to-noise ratio than the commercial PS25255. The total signal-to-noise ratio of the designed electrodes is by 2—14 (4.7) dB higher than that of the commercial PS25255. Such a low SNR of the recorded signal from the PS25255 electrodes may be explained by the modification of the electrode housing as well as by a large contact area and length of the unshielded wire between the electrodes and the skin.

In this research, a schematic diagram of the active electrode for ECG signal acquisition has been developed, model studies of the circuit have been performed, experimental samples of active electrodes have been made and tested.

To verify the actual performance of the circuit, an automated testing system has been built with the use of an oscilloscope, a signal generator and a personal computer running software in Python. The experimental measurements of the parameters of the active electrodes have confirmed the main theoretical conclusions.

Test ECGs have been recorded for a group of people, in the body areas with a low amplitude of the useful signal and a high skin-electrode contact resistance.

The advantages of the obtained electrodes include a low noise and a low signal distortion. This simplifies further processing for useful signal analysis.

The field experiment has confirmed that the goals set in the research have been achieved, as the designed active electrodes may be used in everyday equipment and in wearable electronic devices to record the ECG in the background, without the inconvenience of standard ECG methods.

REFERENCES

1. World Health Organization, Cardiovascular diseases (CVDs). URL: https://www.who.int/news-room/fact-sheets/detail/cardiovascular-diseases-(cvds) (Last accessed: 19.07.21).
2. Searle, A., Kirkup, L. (2000). A direct comparison of wet, dry and insulating bioelectric recording electrodes. *Physiological Measurement*, 21(2), 271–283. https://doi.org/10.1088/0967-3334/21/2/307.
3. Boehm, A., Yu, X., Neu, W., Leonhardt, S., Teichmann, D. (2016). A Novel 12-Lead ECG T-Shirt with Active Electrodes. *Electronics*, 5(4), 1—15. https://doi.org/10.3390/electronics5040075.
4. Huang, J., Cai, Z. (2020). Using Flexible Curved Noncontact Active Electrodes to Monitor Long-Term Heart Rate Variability. *Journal of Healthcare Engineering*, 2020, 1—18. https://doi.org/10.1155/2020/8867712.
5. Peng, S., Xu, K., Bao, S., Yuan, Y., Dai, C., Chen, W. (2021). Flexible Electrodes based Smart Mattress for Monitoring Physiological Signals of Heart and Autonomic Nerves in A Non-Contact Way. *IEEE Sensors Journal*, 21(1), 6—15. https://doi.org/10.1109/JSEN.2020.3012697.
6. Lim, Y. G., Kim, K. K., Park, K. S. (2007). ECG Recording on a Bed During Sleep Without Direct Skin-Contact. *IEEE Transactions on biomedical engineering*, 54(4), 718—725. https://doi.org/10.1109/TBME.2006.889194.
7. Peng, S., Xu, K., Chen, W. (2019). Comparison of Active Electrode Materials for Non-Contact ECG Measurement. *Sensors (Basel)*, 19(16), 1—18. https://doi.org/10.3390/s19163585.
8. Sidikova, M., Martinek, R., Kawala-Sterniuk, A., Ladrova, M., Jaros, R., Danys, L., Simonik, P. (2020) Vital Sign Monitoring in Car Seats Based on Electrocardiography, Ballistocardiography and Seismocardiography: A Review. *Sensors (Basel)*, 20(19), 1—28. https://doi.org/10.3390/s20195699.
9. Jung, S. J., Shin, H. S., Chung, W. Y. (2012). Highly sensitive driver health condition monitoring system using nonintrusive active electrodes. *Sensors and Actuators B: Chemical*, 71–172, 691—698. https://doi.org/10.1016/j.snb.2012.05.056.
10. Geddes, L., Valentinuzzi, M. (1973). Temporal changes in electrode impedance while recording the electrocardiogram with "Dry" electrodes. *Annals of Biomedical Engineering*, 1, 356–367. https://doi.org/10.1007/BF02407675.
11. Han, D. K., Hong, J. H., Shin, J. Y., Lee, T. S. (2009, September). Accelerometer based motion noise analysis of ECG signal. *World Congress on Medical Physics and Biomedical Engineering*, (September 7—12, 2009, Munich, Germany), 198—201. https://doi.org/10.1007/978-3-642-03904-1_56

12. Lee, J., Kim, M., Park, H. K., Young, Kim I. Y. (2020). Motion Artifact Reduction in Wearable Photoplethysmography Based on Multi-Channel Sensors with Multiple Wavelengths. *Sensors (Basel)*, 20(5), 1—14. https://doi.org/10.3390/s20051493.
13. Wiard, R. M., Inan, O. T., Argyres, B., Etemadi, M., Kovacs, G., Giovangrandi, L. (2011). Automatic detection of motion artifacts in the ballistocardiogram measured on a modified bathroom scale. *Medical & Biological Engineering & Computing*, 49(2), 213—220. https://doi.org/10.1007/s11517-010-0722-y.
14. Waller, A. D. (1887) A demonstration on man of electromotive changes accompanying the heart's beat. *The Journal of Physiology*, 8(5), 229—234. https://doi.org/10.1113/jphysiol.1887.sp000257.
15. Lewes, D. (1965). Electrode jelly in electrocardiography. *British Heart Journal*, 27(1), 105—115. https://doi.org/10.1136/hrt.27.1.105.
16. Lopez, A., Richardson, P. C. (1969) Capacitive Electrocardiographic and Bioelectric Electrodes. *IEEE Transactions on Biomedical Engineering*, BME-16(1), 99—99. https://doi.org/10.1109/TBME.1969.4502613.
17. Kosierkiewicz, T. (2013). Dry and Flexible Elastomer Electrodes Outperform Similar Hydrogel and Ag/AgCl Electrodes. *IEEE International Symposium on Medical Measurements and Applications (MeMeA) (4—5 May, 2013, Gatineau, Canada)*, 306-308. https://doi.org/10.1109/MeMeA.2013.6549757.
18. An, X., Stylios, G. K. (2018). A hybrid textile electrode for electrocardiogram (ECG) measurement and motion tracking. *Materials (Basel)*, 11(10), 1—18. https://doi.org/10.3390/ma11101887.
19. Chi, Y. M., Deiss, S. R., Cauwenberghs, G. (2009) Non-contact low power EEG/ECG electrode for high density wearable biopotential sensor networks. *Wearable and implantable body sensor networks, sixth international workshop (5 July, 2009)*, 246—250. https://doi.org/10.1109/BSN.2009.52.
20. Sullivan, T. J., Deiss, S. R., Cauwenberghs, G. (2007, November). A Low-Noise, Non-Contact EEG/ECG Sensor. *IEEE Biomedical Circuits and Systems Conference, (27—30 November, 2007, Montreal, Canada)*, 154—157. https://doi.org/10.1109/BIOCAS.2007.4463332.
21. Prance, R. J., Debray, A., Clark, T. D., Prance, H., Nock, M., Harland, C. J., Clippingdale, A. J., (2000). An ultra low noise electrical-potential probe for human-body scanning. *Measurement Science and Technology*, 11(3), 291—297. https://doi.org/1088/0957-0233/11/3/318.
22. Spinelli, E., Haberman, M. (2010). Insulating electrodes, a review on biopotential front ends for dielectric skin–electrode interfaces. *Physiological Measurement*, 31(10), 183—198. https://doi.org/10.1088/0967-3334/31/10/S03
23. Harland, C. J., Clark, T. D., Prance, R. J. (2002). Electric potential probes—new directions in the remote sensing of the human body. *Measurement Science and Technology*, 13(2), 163—169. https://doi.org/10.1088/0957-0233/13/2/304.
24. Bai, W., Zhu, Z., Li, Y., Liu, L. (2018). A 64.8μW >2.2GΩ DC-AC Configurable CMOS Front-End IC for Wearable ECG Monitoring. *IEEE Sensors Journal*, 18(8), 1—10. https://doi.org/10.1109/JSEN.2018.2809678.
25. He, D. D., Winokur, E. S., Sodini, C. G. (2015). An Ear-Worn Vital Signs Monitor. *IEEE Transactions on Biomedical Engineering*, 62(11), 2547—2552. https://doi.org/10.1109/TBME.2015.2459061.
26. AN5354, Application note. Getting started with the STM32H7 Series MCU 16-bit ADC. URL: https://www.st.com/resource/en/application_note/dm00628458-getting-started-with-the-stm32h7-series-mcu-16bit-adc-stmicroelectronics.pdf (Last accessed: 03.06.21).
27. DS12110 Rev 7, STM32H742xI/G STM32H743xI/G reference manual. URL: https://www.st.com/resource/en/reference_manual/dm00314099-stm32h742-stm32h743753-and-stm32h750-value-line-advanced-armbased-32bit-mcus-stmicroelectronics.pdf (Last accessed: 03.06.21).
28. DocID024030 Rev 7, STM32F427xx/STM32F429xx reference manual. URL: https://www.st.com/resource/en/reference_manual/dm00031020-stm32f405415-stm32f407417-stm32f427437-and-stm32f429439-advanced-armbased-32bit-mcus-stmicroelectronics.pdf (Last accessed: 03.06.21).
29. Kamal, S., Efaz, E. T., Alam, F., Rana, M. (2020). Development of A Low-Cost Real-Time Bioelectrical Signal Acquisition Module. *2nd International Conference on Sustainable Technologies for Industry 4.0 (STI),* (19—20 December 2020, Dhaka, Bangladesh), 1—6. https://doi.org/10.1109/STI50764.2020.9350473.
30. Scher, A. M., Young, A. C. (1960). Frequency Analysis of the Electrocardiogram, *Circulation Research*, 8, 344—346. https://doi.org/10.1589/jpts.25.753.
31. Thakor, N., Webster, J., Tompkins, W. (1984). Estimation of QRS Complex Power Spectra for Design of a QRS Filter. *IEEE Transactions on Biomedical Engineering*, BME-31(11), 702—706. https://doi.org/10.1109/TBME.1984.325393.
32. Pan, J., Tompkins, W. (1985). A Real-Time QRS Detection Algorithm. *IEEE Transactions on Biomedical Engineering*, 32(3), 230—236. https://doi.org/10.1109/TBME.1985.325532.
33. PS25255 EPIC Ultra High Impedance ECG Sensor Advance Information. Data Sheet 291955 issue 1. URL: http://www.saelig.com/supplier/plessey/PS25255.pdf (Last accessed: 03.06.21).

34. A Python program that plots Bode plots of a component using a Rigol DS1054Z Oscilloscope and a JDS6600 DDS Generator. URL: https://github.com/jbtronics/DS1054_BodePlotter (Last accessed: 03.06.21).
35. Kester, W. (2009) Understand SINAD, ENOB, SNR, THD, THD + N, and SFDR so You Don't Get Lost in the Noise Floor. *MT-003 tutorial*. URL: https://www.analog.com/media/en/training-seminars/tutorials/MT-003.pdf (Last accessed: 03.06.21).

Received 03.06.2021
Revised 16.07.2021
Accepted 02.08.2021

А.А. Воропай (https://orcid.org/0000-0002-2783-6700),
В.М. Сарана (https://orcid.org/0000-0002-7778-3176)
Дніпровський національний університет імені Олеся Гончара,
просп. Гагаріна, 72, Дніпро, 49010, Україна,
+380 56 374 9822, cdep@dnu.dp.ua

МАЛОШУМНІ Й ЕКОНОМІЧНІ АКТИВНІ
ЕЛЕКТРОДИ ДЛЯ СУХИХ КОНТАКТНИХ ЕКГ

Вступ. Активні ЕКГ-електроди для натільної електроніки повсякденного використання (окуляри, навушники) дозволяють зробити довгострокову діагностику серцево-судинних захворювань доступною багатьом людям.

Проблематика. Засоби та методи зняття ЕКГ з роками стають доступнішими. Але на шляху до використання їх широким загалом, навіть у випадках коли має значення лише надійна реєстрація R-зубця ЕКГ, є певні труднощі, пов'язані з необхідністю накладати спеціальні електроди (наприклад, хлорсрібні) на певні ділянки тіла через вологі прокладки та виконання конкретних умов або дій з боку людини.

Проблема вирішується використанням сухих електродів, вбудованих у звичні для людини пристрої. Але в цьому випадку низька амплітуда корисного сигналу та великий опір контакту (наприклад, на поверхні голови) не дозволять зняти ЕКГ звичайними засобами.

Мета. Розробка легких у застосуванні натільних ЕКГ-електродів, які можуть бути вбудовані у повсякденні побутові прилади.

Матеріали й методи. Активні електроди на базі гнучких електропровідних матеріалів та високоякісних операційних підсилювачів; методи модельних та експериментальних досліджень для отримання характеристики електронної схеми; метод порівняння з відповідними характеристиками комерційних зразків.

Результати. Розроблено, створено та апробовано прототип активних ЕКГ-електродів, які дозволяють досягти поставленої мети. Отримані результати свідчать про значну роль характеру залежності вхідного реактивного опору від частоти на якість кінцевого сигналу. Для низькоамплітудного ЕКГ сигналу прототип показав на 4.7 дБ краще співвідношення сигнал/шум порівняно з якісними комерційними електродами.

Висновки. Розроблені електроди можуть бути використані у натільних пристроях, на ділянках тіла з низькою амплітудою корисного сигналу та великим опором контакту шкіра–електрод.

Ключові слова: ЕКГ, активні електроди, сухий контакт.